Testis Brain Ribonucleic Acid-Binding Protein/Translin Possesses both Single-Stranded and Double-Stranded Ribonuclease Activities

Jun Wang,[‡] Emily S. Boja,[§] Hammou Oubrahim,[‡] and P. Boon Chock*,[‡]

Laboratory of Biochemistry and Laboratory of Biophysical Chemistry, National Heart, Lung, and Blood Institute, National Institutes of Health, Bethesda, Maryland 20892-8012

Received June 4, 2004; Revised Manuscript Received July 19, 2004

ABSTRACT: RNA interference (RNAi) is a biological process in which animal and plant cells destroy double-stranded RNA (dsRNA) and consequently the mRNA that shares sequence homology to the dsRNA. Although it is known that the enzyme Dicer is responsible for the digestion of dsRNA into ∼22 bp fragments, the mechanism through which these fragments are associated with the RNA-induced silencing complex (RISC) is mostly unknown. To find protein components in RISC that interact with the ∼22 bp fragment, we synthesized a ^{32}P- and photoaffinity moiety-labeled 22 bp dsRNA fragment and used it as bait to fish out protein(s) directly interacting with the dsRNA fragment. One of the proteins that we discovered by mass spectrometric analysis was TB-RBP/translin. Further analysis of this DNA/RNA binding protein showed that it possesses both ssRNase and dsRNase activities but not DNase activity. The protein processes long dsRNA mainly into ∼25 bp fragments by binding to the open ends of dsRNA and cutting it with almost no turnover due to its high affinity toward the products. The activity requires physiological ionic strength. However, with single-stranded RNA as substrate, the digestion appeared to be more complete. Both ssRNase and dsRNase activities are inhibited by high levels of common RNase inhibitors. Interestingly, both activities can be enhanced greatly by EDTA.

Animal and plant cells have a mechanism to degrade double-stranded RNA (dsRNA) with a concomitant degradation of mRNA of corresponding sequence. This phenomenon, called RNA interference (RNAi)[1] (*1*−*4*), provides a new tool for protein knockdown by eliminating its mRNA and is already widely used today in protein functional studies since its discovery a decade ago (*5*, *6*). Great interest has also been aroused for the potential therapeutic applications of the method to diseases, such as cancer and infections (*7*, *8*).

In *Caenorhabditis elegans* and *Drosophila*, uptake of dsRNA as long as a few hundred base pairs leads to specific gene silencing (*9*−*12*). However, in many mammalian cells shorter dsRNA fragments (∼22 bp) work much better than longer dsRNA, which often results in nonspecific gene inactivation (*13*−*15*), although it has been shown in certain mammalian cells that longer dsRNA leads to effective specific gene silencing (*16*, *17*). Sledz et al. showed that both nonspecific gene silencing by long dsRNA and specific gene silencing by shorter dsRNA are accompanied by activation of the INFγ pathway, thus substantiating the speculation that the degradation of dsRNA and the corresponding mRNA is a mechanism that defends cells from foreign agents, such as viruses and transposons (*18*). In addition to this defense mechanism, short dsRNA fragments (∼22 bp) generated from endogenous stem−loop precursors, e.g., microRNA (miRNA), also lead to mRNA destruction (*19*). Although the functions of most miRNA are unknown, it is believed that they are used for gene regulation. For example, miRNA lin4 and let7 from *C. elegans* inhibit protein synthesis by binding to the 3′ untranslated region (UTR) of target mRNA. Others, such as the scarecrow protein found in plants, act like siRNA to destroy the target transcript (*20*). Unlike normal mRNA turnover that takes place mostly in the nucleus and is carried out mostly by exo-RNases (*21*), this degradation of mRNA through dsRNA happens in the cytoplasm and must require a unique pathway.

Indeed, mechanistic studies revealed that when dsRNA enters a cell, it is first digested into ∼22 bp short dsRNA (small interference RNA or siRNA) by Dicer, a RNase III family member that is also responsible for miRNA formation. siRNA fragments, usually 5′-phosphorylated, then bind to the RNA-induced silencing complex (RISC) where they are unwound and directed to mRNA (using the antisense strand) (*1*−*4*, *22*, *23*). In *C. elegans*, the short antisense strand annealed to mRNA is elongated using the mRNA as a template by a RNA polymerase to form a longer dsRNA that, upon cleavage again into ∼22 bp dsRNA fragments, greatly amplifies the signal and leads to highly efficient RNA silencing (*24*). In higher organisms, such as mammalian cells, such signal amplification was not found. However, by

* To whom correspondence should be addressed at LB/NHLBI/NIH, Building 50, Room 2134, 50 South Drive, MSC-8012, Bethesda, MD 20892-8012. Tel: 301-496-2073. Fax: 301-496-0599. E-mail: bchock@nih.gov.

[‡] Laboratory of Biochemistry, NHLBI.

[§] Laboratory of Biophysical Chemistry, NHLBI.

[1] Abbreviations: 4-S-U, 4-thiouridine; TB-RBP, testis brain ribonucleic acid-binding protein; ss, single stranded; ds, double stranded; RNAi, RNA interference; RISC, RNA-induced silencing complex; UTR, untranslated region; miRNA, microRNA; siRNA, small interference RNA; IEF, isoelectric focusing; EDTA, ethylenediaminetetraacetic acid; QTOF, quadruple time of flight; CID, collision-induced dissociation; ATPγS, adenosine 5′-[γ-thio]triphosphate; GTPγS, guanosine 5′-[γ-thio]triphosphate; AMP-PNP, adenosine 5′-[β,γ-imido]triphosphate.

10.1021/bi048847l
Published on Web 09/28/2004

introducing many copies of siRNA or small numbers of longer dsRNA, gene silencing can reach satisfactory levels, although in certain cell types, longer dsRNA leads to nonspecific gene silencing (*13*−*15*).

The least well understood mechanism of the RNAi pathway lies in RISC. What is this protein complex composed of? How the dsRNA is unzipped and how it is directed to mRNA are issues that need to be resolved. One of the components of RISC is Argonaute2, which is believed to bind to the 3′ overhang of siRNA through a PAZ domain capable of binding single-stranded RNA with relatively low affinity (*25*, *26*). Other components of RISC are not well established.

Testis brain RNA-binding protein (TB-RBP) is a 28 kDa DNA/mRNA binding protein first discovered in mouse testis and brain, where it binds to the 3′ untranslated region (UTR) of translationally regulated mRNA encoding proteins such as protamine 1, protamine 2, and transition protein 1 (*27*−*29*). Later it was found to be expressed ubiquitously (*30*). The amino acid (aa) sequence of TB-RBP is 99% identical to its human counterpart, translin, with only a 3 aa difference out of 228 aa (thus, TB-RBP and translin are used interchangeably). The physiological role of this protein is not well understood. Translin is implicated in binding to consensus sequences at breakpoint junctions of chromosomal translocations in lymphoid tumors and at recombination hot spots during meiosis in germ cells (*31*−*35*). Since it accumulates in the nuclei of male germ cells during meiosis, it may play a role in DNA recombination. As a RNA-binding protein, translin binds to conserved Y and H elements of many brain and testis mRNAs (*28*, *36*, *37*). It has been suggested to be involved in RNA transport and storage because it has the ability of linking translationally suppressed mRNA to microtubules and releasing bound mRNAs following disassociation of microtubules (*36*, *37*). TB-RBP has also been shown to move between nuclei and cytoplasm in male germ cells, suggesting a mRNA transporting function (*38*, *39*).

In vitro studies revealed that the protein has very high affinity toward double-stranded DNA (dsDNA) with K_d ranging from 15 to 90 nM (*40*, *41*). Both electron microscopic (*42*) and X-ray crystallographic (*43*) analyses, as well as ultracentrifugation (*40*) and fluorescence (*44*) studies, have shown that the protein exists as an octamer that organizes into an elongated spherical particle with a large cavity in its center to bind DNA or RNA.

TB-RBP contains a putative GTP-binding site that is not shown in the X-ray crystal structure. However, site-directed mutagenesis aimed at abolishing the GTP-binding ability yielded a mutant that no longer binds to RNA, yet its ability to bind DNA remains intact. Transfection of this mutant protein into NIH3T3 cells leads to high cell death rate, indicating the importance of this domain (*45*). Interestingly, mice with knocked-out TB-RBP were viable but showed a coordinated loss of TRAX, a TB-RBP binding protein, and reduced fertility and probably muscle strength. In addition, altered gene expression in the brain and behavioral changes were also observed (*46*, *47*).

TB-RBP's wide-range involvement in biological processes indicates that it is likely a highly regulated protein. Indeed, the crystal structure of the octamer reveals a large surface area accessible for binding regulatory proteins (*43*). However, to date, the best characterized protein that interacts with TB-RBP is TRAX, a 33 kDa protein sharing extensive amino acid homology to TB-RBP with unknown function (*48*).

Here we report that, during our attempt to "fish out" a potential component that binds dsRNA or siRNA in RISC, a protein tightly bound to siRNA was discovered and identified to be TB-RBP. Characterization studies with the *Escherichia coli* overexpressed protein revealed that TB-RBP possesses both ssRNase and dsRNase activities. The digestion sites are at two open ends of dsRNA and likely also at those of ssRNA. The turnover rates for the digestion are very low due to strong product inhibition.

EXPERIMENTAL PROCEDURES

Materials. [α-^{32}P]GTP was from Amersham-Pharmacia. 4-Thiouridine (4-S-U) was from Trilink. mRNA and the dsRNA synthesis kit were from Ambion (T7-MEGAshortscript high-yield transcription kit). Proteinase K and RNase inhibitor mixtures were from Promega. NuPAGE gels, TBE gels, IEF gels, and PVDF membranes were from Invitrogen. pET-22b vector was from Novagen. Super-flow Ni resin was from Qiagen, while Resource-S, Resource-Q, and Superdex-200 were from Amersham-Pharmacia. Protease inhibitor cocktails without EDTA (complete, mini) were purchased from Roche. The mice cDNA library was from Clontech. Other chemicals were purchased from Sigma-Aldrich. All materials used were free of RNases.

Construction of pET-22b TB-RBP. cDNA of mouse TB-RBP was cloned from the mouse testis cDNA library by PCR using primers 5′-gcgcggatccgatgtctgtgagcgagatcttcgtg-3′ and 5′-atatgcggccgcttttttcaccacaagccgctgctgt-3′ containing *Bam*HI and *Not*I sites (underlined), respectively. The PCR fragment was digested with the respective enzymes and inserted into the pET-22b vector.

Overexpression and Purification of His6-TB-RBP. His6-TB-RBP was overexpressed in *E. coli* [BL21(DE3)] in a 10 L fermenter using the standard protocol. The cell pellet (75 g) was suspended in 100 mL of buffer C (25 mM Tris-HCl, pH 7.4, 100 mM NaCl, 0.5% Triton X-100, and protease inhibitors without EDTA) followed by French press treatment. The cell lysate thus obtained was centrifuged at 12 krpm in an ss-34 rotor for 30 min, and the supernatant was loaded onto a Ni column (3 cm long × 2.6 cm wide). His6 translin was eluted from the column according to the QIAGEN protocol.

Translin purified from the Ni column, after being dialyzed against 25 mM Tris-HCl, pH 7.4, and 10 mM β-mercaptoethanol to get rid of most of the salt and imidazole, was further purified on a Resource-S column (10 cm long × 2.6 cm diameter) using a 10−500 mM NaCl gradient in 5 mM β-mercaptoethanol and 25 mM Tris-HCl buffered at pH 7.5. The TB-RBP portion collected was loaded onto a Resource-Q column (10 cm long x 2.6 cm diameter) and eluted with the same conditions as described for the Resource-S procedure. The final purification step was performed on a Superdex-200 gel filtration column (90 cm long × 2.6 cm diameter), with TB-RBP eluted with 20 mM Tris-HCl, pH 7.4, buffer containing 100 mM NaCl, 10 mM β-mercaptoethanol, and 0.05% Triton X-100. The HPLC used for the purification was a Hewlett-Packard 1100 series system with a Pharmacia

LKB RediFrac collector. The purified TB-RBP was stored in the presence of 50% glycerol at −20 °C.

Synthesis of ^{32}P- and 4-S-U-Labeled siRNA. The protocol of the Ambion Megashortscript siRNA kit was followed. For the DNA template, the following primers were used: forward, 5′-aaccgcgcggccgcccgggcc*cctgtctc*-3′, and backward, 5′-aaggcccgggcggccgcgcgg*cctgtctc*-3′ (italic letters indicate the T7 promoter region). During the synthesis of ^{32}P-4-S-U-labeled siRNA, [α-^{32}P]GTP was added to a final concentration of 1 mCi/mL. The final nucleoside triphosphate concentration, including that of 4-S-U triphosphate, was ∼20 mM each.

Preparation of the Cell Lysate. NIH3T3 cells grown in four 15 cm dishes to near confluency were trypsinized and washed with buffer A (250 mM sucrose, 1 mM $MgCl_2$, 5 mM sodium phosphate buffer, pH 7.1) and homogenized with a cell homogenizer in 300 μL of buffer B [2 mM $MgCl_2$, 100 mM NaCl, 30% (v/v) glycerol, 10 mM Tris-HCl, pH 7.4, and complete protease inhibitor cocktails without EDTA]. After centrifugation at 10 krpm in a Biofuge Fresco benchtop centrifuge, the soluble fraction was used for the photoaffinity labeling experiment.

Photoaffinity Labeling Experiment. The cell lysate prepared above (40 μL) was mixed with 5 μL of [^{32}P]-4-S-U-labeled siRNA (ca. 0.2 μM final concentration) and 2.5 μL each of GTPγS and AMP-PNP (final concentration 500 μM). The mixture was irradiated at 0 °C with 365 and 254 nm UV light for 10 min (5 min each) using a hand-held UV lamp (with 4 W UV bulbs), followed by native IEF and NuPAGE gel electrophoresis. The 2D gel was blotted on a PVDF membrane that was used for radiography and Coomassie Blue staining.

RNase Activity Assays. Translin (final concentration 42 μM) was mixed with ssRNA (final concentration 6 μM or 30 nM) or dsRNA (final concentration 3 μM or 15 nM) and 10× buffer (final concentrations: 100 mM NaCl, 25 mM HEPES, pH 7.5, 2 mM $MgCl_2$) in the presence or absence of RNase inhibitors (final concentrations 80 units), in the presence or absence of ATP/ATPγS and GTP/GTPγS (concentration 500 μM), or in the presence or absence of EDTA (final concentration 5 mM, and in this case, the 10× buffer was without $MgCl_2$). In experiments where the effects of metal ions were tested, the final concentrations of $CaCl_2$, $MnCl_2$, $ZnCl_2$, $FeCl_3$, and $CuCl_2$ were 1 mM [although at pH 7.5, $FeCl_3$ is converted to $Fe(OH)_3$, $FeCl_4^-$, etc. with only $\sim 2 \times 10^{-12}$ μM free Fe^{3+} and $CuCl_2$ to $Cu(OH)_2$ with ∼2 μM free Cu^{2+}]. The mixture was incubated at 37 °C, and a 20 μL sample was drawn and cooled to −80 °C at different time intervals. After the incubation period, 20 μg of proteinase K was added to each thawed sample, and the mixtures were incubated at 37 °C for 1 h before being loaded onto a 12% NuPAGE gel or TBE gel for electrophoresis. The gel was dried and used for radiography or stained with ethidium bromide for UV visualization.

LC-MS/MS Analysis of Labeled Proteins. Radioactively labeled protein spot stained with Coomassie Blue was excised, reduced, and alkylated, followed by trypsinization as previously described (*49*). The digests were analyzed on a Micromass QTOF Ultima Global (Micromass, Manchester, U.K.) in electrospray mode interfaced with an Agilent HP1100 CapLC (Agilent Technologies, Palo Alto, CA) prior to the use of the mass spectrometer. Five microliters of each digest was loaded onto a Vydec C_{18} MS column (100 × 0.15 mm; Grace Vydec, Hesperia, CA), and chromatographic separation was performed at 1 μL/min using the following gradient: 0−10% solvent B over 5 min; 10−40% solvent B over 60 min; 40−95% solvent B over 5 min; 95% solvent B held for 5 min (solvent A, 0.2% formic acid in water; solvent B, 0.2% formic acid in acetonitrile). A data-dependent analysis (DDA) method collected collision-induced dissociation (CID) data for the three most abundant multiply charged ions observed in the preceding survey scan (*m*/*z* 300−1990) above a threshold of 10 counts/s. Data were processed using MassLynx software (version 3.5) to generate peak list files before submitting them to an in-house licensed Mascot search at http://biospec.nih.gov (MatrixScience Ltd., London, U.K.). Peptide and MS/MS tolerances were set at ±0.2 Da. All MS/MS fragment ions were within 50 ppm of their theoretical values.

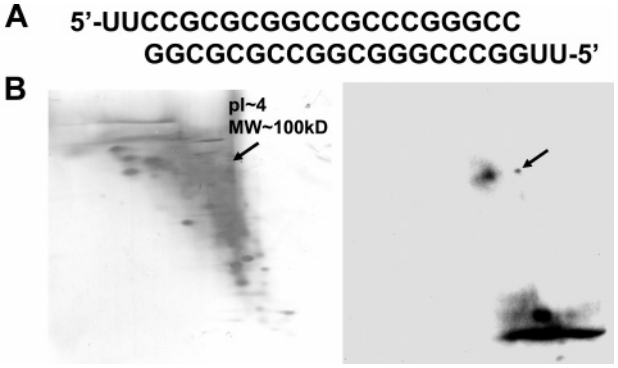

FIGURE 1: Phtoaffinity labeling of proteins that interact with 22 bp siRNA. NIH3T3 cell lysate (cytosolic) was added ^{32}P- and 4-S-U-labeled siRNA (A) in the presence of 500 μM each of GTPγS and AMP-PNP as described in Experimental Procedures. The mixture was irradiated with 365 and 254 nm UV light (5 min each) before it was subjected to 2D gel separation under native conditions. The radiography of the 2D gel showed one protein spot that was radioactively labeled (arrow in panel B, right). The Coomassie Blue stained gel is shown on the left panel.

RESULTS

TB-RBP/Translin Binds siRNA with High Affinity. To obtain protein(s) that directly interact with siRNA, we synthesized a ^{32}P-labeled 22 bp dsRNA with two 4-S-U residues hanging out at both 5′ ends (Figure 1A). 4-S-U is known as a photoaffinity labeling moiety, which upon UV irradiation will form covalent linkage to adjacent molecules (*50*). The siRNA (ca. 0.2 μM final concentration) was mixed with the NIH3T3 cell lysate (cytosolic) in the presence of 0.5 mM each of GTPγS and AMP-PNP and was irradiated for 5 min with 365 nm and 5 min with 254 nm UV light. After 2D gel electrophoresis of the treated cell lysate under native conditions, we found only one protein spot that was radioactively labeled (Figure 1B, right panel, indicated by arrow). The bigger spot to the left is due to nonspecific contamination during blotting). This protein spot, which appeared at pH 5 and had an apparent MW of ∼120 kDa as shown in the Coomassie Blue stained 2D gel (Figure 1B, left panel), was cut from the gel and rendered for MS analysis. Trypsinization followed by tandem MS/MS analysis of the protein yielded nine peptide fragments that matched the mouse TB-RBP (Figure 2B, Table 1) in the NCBInr database using the Mascot search engine. Table 1 lists the

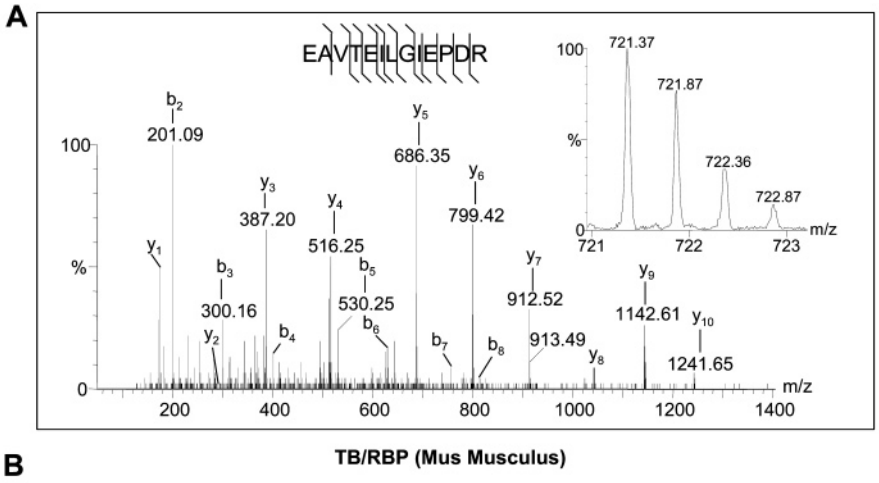

FIGURE 2: MS analysis of the ^{32}P-labeled, siRNA-containing protein revealed it to be TB-RBP/translin. (A) CID spectrum of the +2 charged precursor ion at *m*/*z* 721.37 corresponding to the sequence in the inset. (B) TB-RBP/translin sequence presented with the residues identified in the peptide fragments (italic) shown in Table 1.

Table 1: MS/MS Analysis of Mouse ^{32}P-Labeled siRNA-Bound Protein[a]

residue	sequence	obsd *m*/*z* (Da)	M_r (exptl)	M_r (calcd)	Δ (Da)
4−14	(R)KVVQSLEQTAR	629.85	1257.68	1257.70	−0.02
5−14	VVQSLEQTAR	565.80	1129.58	1129.61	−0.03
15−34	EILTLLQGVHQGTGFQDIPK	732.05	2193.12	2193.18	−0.06
41−47	EHFSTVK	434.21	846.41	846.42	−0.01
48−54	THLTSLK	400.23	798.45	798.46	−0.01
57−64	FPAEQYYR	537.25	1072.48	1072.50	−0.02
95−107	EAVTEILGIEPDR	721.37	1440.72	1440.75	−0.03
95−109	EAVTEILGIEPDREK	849.93	1697.85	1697.88	−0.03
182−193	(K)KVEEVVYDLSIR	725.39	1448.76	1448.79	−0.03

[a] The sequences of nine peptide fragments determined by MS/MS analysis are listed with the residue number corresponding to the sequence of TB-RBP/translin shown in Figure 2B.

nine peptide fragments revealed by MS/MS analysis. Figure 2A shows one example of the CID spectrum of a tryptic peptide, ^{95}EAVTEILGIEPDR^{107}, with its precursor ion at *m*/*z* 721.37^{2+}. The presence of y_1-y_{10} as well as b_2-b_8 ions confirms the sequence. The sequence of the nine peptide fragments matches well with that of TB-RBP shown in Figure 2B, with the identified residues in italic font.

Purification and Partial Characterization of Overexpressed TB-RBP/Translin. To study the involvement of TB-RBP in RNAi, we overexpressed this protein in *E. coli* using the expression vector pET-22b. This vector allows the protein to be secreted into the periplasm of *E. coli* for proper folding. The leading sequence for the secretion is digested after the protein is in the periplasm. For purification purposes, the overexpressed protein contains a His6 tag at its C-terminus.

TB-RBP overexpressed from *E. coli* was extensively purified to remove possible RNase contamination that would interfere with the activity test described below (also, see Discussion). After the His6-TB-RBP from the crude cell lysate was eluted from the Ni column, it was dialyzed against 25 mM Tris-HCl, pH 7.5, and 10 mM β-mercaptoethanol before it was further purified on three consecutive columns: cation-exchange Resource-S, anion-exchange Resource-Q, and size-exclusion Superdex-200. The protein was purified to homogeneity after the four columns, as indicated by both Coomassie Blue (Figure 3A) and silver staining (data not shown). It is interesting to note that, even in the presence of

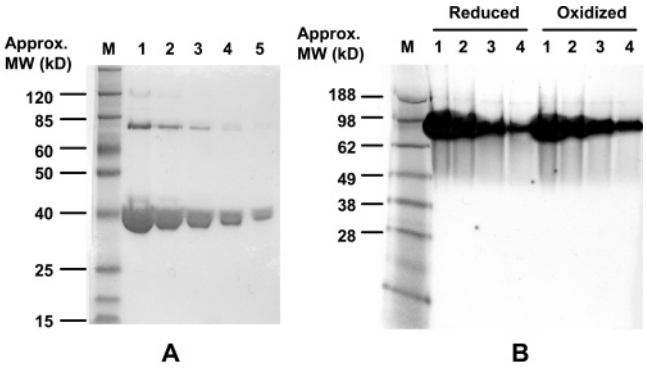

FIGURE 3: Extensive purification of overexpressed TB-RBP. The His6-labeled protein was overexpressed in *E. coli.* After four columns (Ni, Resource-S, Resource-Q, and Superdex-200, respectively), the protein was purified into homogeneity. On SDS gel and in the presence of 10 mM β-mercaptoethanol (A), the protein exists mainly in monomer with small amounts of dimer and trimer (from lanes 1 to 5, the amount of protein loaded was 24, 12, 6, 3, and 1.5 μg, respectively). On native gel (B), the protein shows only one band in the presence (reduced) or absence (oxidized) of 10 mM β-mercaptoethanol (from lanes 1 to 4, the amount of protein loaded was 24, 12, 6, and 3 μg, respectively). Lanes M in panels A and B show the mobility of Bench Marker and See Blue Plus 2, respectively, under the conditions described for each panel.

10 mM β-mercaptoethanol as reducing agent, the protein shows dimer (Figure 3A, lanes 1−3, ~80 kDa) and trimer bands (Figure 3A, lane 1, ~120 kDa) on the SDS−PAGE

gel, indicating that interactions beyond disulfide bonds exist between protein subunits. However, the protein shows only one band on the native gel regardless of reduced or oxidized conditions (Figure 3B). Since the previous report indicated that translin can form intermolecular disulfide bonds using Cys225 (*44*), we decided to analyze the disulfide linkages of the dimeric translin by MS analysis. In-gel trypsinization of this protein indeed revealed the disulfide bond described above as we observed the +2 and +3 charges of disulfide-bonded peptide ^{220}ETAAA$\underline{C}$GEK^{228}-^{220}ETAAA$\underline{C}$GEK^{228} at *m*/*z* 878.39 and 585.93 ($\overline{MH}^+$ 1755.77; data not shown). Interestingly, two more disulfide linkages were found between Cys58−Cys225 (MH^+ 1239.58) and Cys58−Cys58 (MH^+ 723.38). These covalent bonding patterns likely contribute to the formation of the octamer previously observed.

TB-RBP/Translin Exhibits dsRNase and ssRNase Activities. To investigate the potential role of TB-RBP/translin in RNAi, the purified protein was used to study its DNA/RNA binding and processing activities. As reported, the protein shows tight double-stranded DNA (dsDNA) and single-stranded RNA (ssRNA) binding abilities, as the protein−nucleic acid complexes comigrate on SDS or native acrylamide gels (data not shown). In addition, we found that it also binds double-stranded RNA well (see below). Since TB-RBP interacts with both ssRNA and dsRNA, we investigated whether it can unwind dsRNA and direct one strand (antisense) to the corresponding ssRNA (mRNA). After TB-RBP (final monomer concentration 4.2 μM) was incubated at 37 °C with a mixture of 100 base long ssRNA (final concentration ca. 3 μM) and short, ^{32}P-labeled dsRNA (whose sequence is part of that of the long ssRNA, final concentration ca. 3 μM) in the presence of ATP or GTP, gel electrophoresis did not show the annealing of the ^{32}P-labeled antisence patch to the 100 base ssRNA (data not shown).

We then checked to see if TB-RBP can process dsRNA longer than 25 bp. When the protein (final monomer concentration 42 μM) was mixed with 500 bp long, ^{32}P-labeled dsRNA (final concentration 3 μM) and incubated at 37 °C for 20 h under various conditions, we observed that the protein can cut dsRNA into ~25 bp fragments (Figure 4). It is noteworthy that the activity of TB-RBP requires a certain ionic strength. By comparing it to the synthetic 25 bp dsRNA (lane M) and the uncut 500 bp dsRNA as control (lane 1), we found that the digestion did not occur when the reaction mixture was deprived of ions (lane 2). However, in the presence of 100 mM NaCl (lane 3), the protein can cut dsRNA into ~25 bp fragments. Introduction of 1 mM each of Mg^{2+}, Ca^{2+}, Mn^{2+}, or Zn^{2+} in addition to 100 mM NaCl showed no significant effect on the cutting rate (lanes 4, 5, 6, and 7, respectively). However, a 1 mM final concentration of $FeCl_3$ or $CuCl_2$ (at pH 7.5 $FeCl_3$ is converted to $Fe(OH)_3$, $FeCl_4^-$, etc. with negligible [Fe^{3+}] and $CuCl_2$ is converted to $Cu(OH)_2$ with [Cu^{2+}] ~2 μM) inhibited the protein activity (lanes 8 and 9, respectively). However, the turnover rate is so low that, in order to see the 25 bp bands clearly, the film in Figure 4 was highly overexposed. This low turnover rate was expected due to the high affinity between the product and the protein.

To separate the products from TB-RBP after the reaction, we treated the reaction mixtures with proteinase K that destroyed TB-RBP and released the 25 bp products. In these experiments, as shown in Figure 5 (ethidium bromide stained agarose gels), we found that TB-RBP possesses both ssRNase and dsRNase activities. Results indicate that when nucleic acids (final concentrations 15 nM dsRNA and 30 nM ssRNA) were mixed with TB-RBP (final concentration 42 μM) for 24 h before proteinase K treatment, 500 base ssRNA, as well as 500 bp dsRNA, was degraded in the presence of any of the following nucleotides at 0.5 mM: ATP, GTP, ATPγS, or GTPγS (lanes 2−5, respectively). Loaded in lane 1 in panels A and B of Figure 5 are ssRNA and dsRNA, respectively, without TB-RBP digestion, used as controls. Note that mobility of the 500 base ssRNA is much slower than that of 500 bp dsRNA. Products of ssRNase showed a smear on the gel, indicating a relatively nonspecific cutting (Figure 5A, lanes 2−5), while those of dsRNase were ~25 bp fragments that were too weak to be visualized by ethidium bromide staining (Figure 5B, lanes 2−5; for 25 bp products

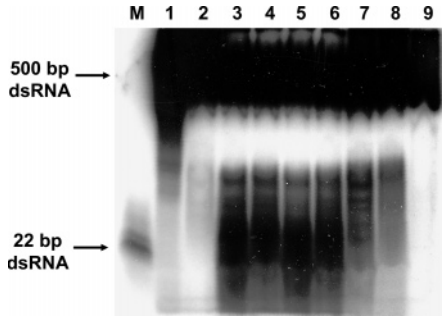

FIGURE 4: TB-RBP processes 500 bp dsRNA into ~25 bp fragments. TB-RBP was mixed with ^{32}P-labeled 500 bp dsRNA in a molecular ratio of ~10:1 and incubated at 37 °C in 25 mM HEPES, pH 7.5, for 20 h under indicated concentrations of mono- or divalent metal ions: no salt (lane 2), 100 mM NaCl (lane 3), and, in addition to 100 mM NaCl, 1 mM $MgCl_2$ (lane 4), 1 mM $CaCl_2$ (lane 5), 1 mM $MnCl_2$ (lane 6), 1 mM $ZnCl_2$ (lane 7), saturated $FeCl_3$ (lane 8), and saturated $CuCl_2$ (lane 9) (described in Experimental Procedures). By comparison to the synthetic ^{32}P-labeled 22 bp siRNA as a marker (lane M), TB-RBP can cut dsRNA into ~25 bp fragments in physiological salt concentrations, but Zn^{2+}, Fe^{3+}, and Cu^{2+} can abolish the dsRNase activity. Loaded on lane 1 was the 500 bp dsRNA alone.

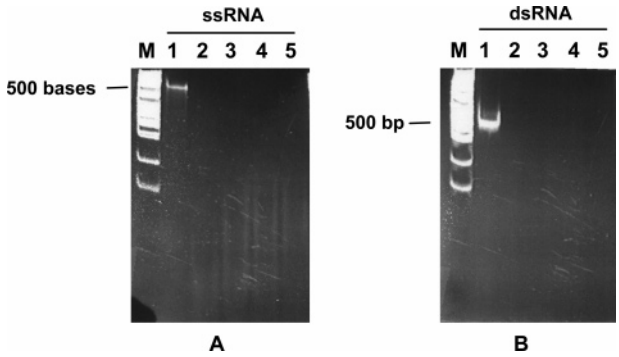

FIGURE 5: TB-RBP possesses both ssRNase and dsRNase activities. A large excess of TB-RBP (42 μM, or 5.25 μM octamer) was incubated with ssRNA (panel A, 30 nM) or dsRNA (panel B, 15 nM) in 100 mM NaCl and 25 mM HEPES, pH 7.4, in the presence of 0.5 mM ATP (lane 2), 0.5 mM GTP (lane 3), 0.5 mM ATPγS (lane 4), and 0.5 mM GTPγS (lane 5) and incubated at 37 °C for 24 h before being treated with proteinase K. The mixtures were then loaded onto a 1% agarose gel, and after electrophoresis, the nucleic acid bands were visualized by ethidium bromide staining. Lane 1: ssRNA (A) or dsRNA (B) untreated with TB-RBP but with proteinase K.

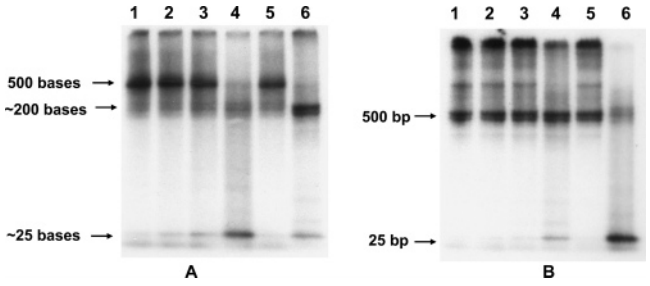

FIGURE 6: An autoradiograph of the time course of ssRNase (A) and dsRNase (B) activities of TB-RBP shows very slow reaction rates. TB-RBP (42 μM, or 5.25 μM octamer) and ^{32}P-labeled ssRNA (3 μM) or ^{32}P-labeled dsRNA (1.5 μM) were incubated at 37 °C for 0, 1, 3, and 20 h (lanes 1, 2, 3, and 4, respectively) in 100 mM NaCl in 25 mM HEPES, pH 7.4, before proteinase K treatment to destroy the protein. The mixtures were then loaded onto a 12% NuPAGE gel for electrophoresis and subsequent autoradiographic visualization. Both ssRNA and dsRNA yielded ~25 bp products but different parental molecules: ~200 base product for ssRNA and ~450 bp product for dsRNA. RNase inhibitor cocktail inhibits both ssRNase and dsRNase activities (lane 5) as 20 h incubation did not lead to product formation. 5 mM EDTA accelerates both ssRNase and dsRNase activities (lane 6, 20 h incubation).

radioactively labeled, see Figures 4 and 6). Similar experiments indicate that the protein does not process dsDNA or ssDNA (data not shown).

Because TB-RBP binds tightly to ~25 bp dsRNA fragments, it is conceivable that the turnover rates of its ssRNase and dsRNase activities are low (near unity) due to product inhibition. Indeed, when nearly stoichiometric amounts of ssRNA or dsRNA were mixed with TB-RBP (nucleic acid: protein octamer ~1.75:3.5), after proteinase K digestion, only an equivalent amount of dsRNA was cut into ~25 bp fragments after 20 h of incubation (Figure 6B, lane 4). It has been reported that TB-RBP/translin binds only to the open ends of DNA (*40*). In this case, we speculate that the protein binds only to the open ends of dsRNA and then cuts ~25 bp fragments from them, releasing a shorter parental dsRNA of ~450 bp (compare lane 4 to lane 1 of Figure 5B). On the contrary, there are turnovers for ssRNA (Figure 6A). After 20 h reaction, the 500 base ssRNA was converted mostly to products with apparent MW ~200 base and ~25 bp (Figure 6A, lane 4). The smear pattern may indicate a certain degree of nonspecificity of TB-RBP binding and digestion. It is noteworthy that TB-RBP activities were inhibited by a mixture of RNase inhibitors, indicating that the protein possesses a known RNA digestion mechanism (Figure 6, lanes 5). Interestingly, the ssRNase and dsRNase activities were greatly altered by 5 mM EDTA (lanes 6, Figure 6) for reasons still under investigation: while dsRNase activity was enhanced (lane 6, Figure 6B), the ssRNase activity was changed to produce mostly a ~200 base fragment (lane 6, Figure 6A). Here, the different activities of the protein toward ssRNA and dsRNA were again observed: while it cuts dsRNA into ~25 bp fragments, it only processes ssRNA into larger products, with an apparent MW of ~200 bases and ~25 bp.

DISCUSSION

During our search for a RISC protein(s) that directly interacts with siRNA, a 22 bp siRNA labeled with ^{32}P and a photoaffinity moiety, 4-thiouridine, was synthesized and used to label any protein that binds siRNA with reasonable affinity. From the mouse NIH3T3 cell lysate (cytosolic), we found one such labeled protein identified by MS analysis to be TB-RBP whose human analogue is translin (Figures 1 and 2).

To investigate its functional role as a potential component of RISC, the extensively purified, *E. coli* overexpressed protein was found to possess both ssRNase and dsRNase activities (Figures 5 and 6). Under nearly physiological conditions (100 mM NaCl, pH 7.4), the protein can process 500 bp dsRNA into ~25 bp fragments from both open ends with single turnover due to product inhibition. ssRNA can also be processed into longer and shorter fragments (mainly with an apparent molecular weight of ~200 bases and ~25 bp) with a higher turnover number. Since ssRNA has secondary structures, it is difficult to predict the specificity of TB-RBP toward ssRNA. These activities are not due to contamination of other RNases because (1) the protein overexpressed in *E. coli* was purified extensively, (2) the newly purified protein did not show such activities unless stored at −20 °C in glycerol for a few days, indicating that proper folding/reorganization of the protein is necessary (data not shown), and (3) unlike low molecular weight RNases that digest RNA into single nucleotides, TB-RBP cuts ssRNA and dsRNA with a certain pattern and, in the case of dsRNA digestion, the ~25 bp products are released from TB-RBP only when the protein is proteolyzed, such as digestion by proteinase K. Mechanisms of the TB-RBP RNase activities remain a mystery because the X-ray structure of the protein does not show traditional RNase foldings (*43*). However, it is possible that upon binding the lower local pH near the P−O linkage can make this bond scissile to water attack. But to illustrate this point, a detailed structure of the TB-RBP−RNA complex is desired. It should be pointed out that the purified TB-RBP fails to process DNA.

TB-RBP has been shown to bind DNA with high affinity (*40*, *41*). Under physiological conditions, this protein is an octamer, as shown by various methods (*40*, *42*−*44*). However, there are discrepancies between the octamer structures reported: the X-ray structure indicates a head-to-tail organization between each unit while electromicroscopy shows a head-to-head linkage. This difference could be due to the different protein sources used in the experiments. Our MS analysis of the protein showed disulfide linkage between C58 and C225, in addition to that between C225 and C225 reported elsewhere (*44*). With so many functions known to TB-RBP so far, it is not surprising to see different organizations of the octamer structures that may carry out different tasks in vivo. In both X-ray and electromicroscopic structures, eight subunits cluster to form a barrel encircling a cavity into which DNA or RNA can bind (*42*, *43*). Although, from the primary structure, the protein contains a putative GTP-binding domain and mutation of this domain has shown a negative predominant effect on cell growth (*45*, *46*), the X-ray structure does not show a secondary structure of the GTP- or ATP-binding domain (*43*). This is consistent with our results that TB-RBP can digest ssRNA or dsRNA without ATP, GTP, or their nonhydrolyzable analogues (Figures 5 and 6). Also, in the presence or absence of ATP/GTP, we did not observe that the protein alone can catalyze the annealing of the antisense strand of dsRNA to its corresponding mRNA.

Translin has been implicated to be involved in many biological processes, from RNA transporting to transcription regulation (*27*−*39*). In this paper, we show that it can digest both ssRNA and dsRNA. The digestion of dsRNA yields ∼25 bp products. This activity is reminiscent of Dicer, an RNase III family member that is involved in RNAi by cutting dsRNA into ∼22 bp fragments (*1*−*4*). Whether TB-RBP is actively involved in RNAi is under investigation. It has also yet to be determined if the protein is a part of RISC. But due to its high affinity to the 25 bp products, we show that the turnover rate of TB-RBP in the hydrolysis of dsRNA is so low that only when the protein is proteolyzed by a protease can the products be released. In fact, TB-RBP shows high affinity not only toward the 25 bp dsRNA fragments but also to longer RNA or DNA molecules. As reported, this affinity is due to the binding of TB-RBP/translin to the open ends of the nucleic acids (*41*), although both X-ray and microscopic structures failed to explain why this is the case (*42*, *43*). This notion is demonstrated in our experiments in that, instead of cutting 500 bp dsRNA into fragments of numerous lengths as predicted by random binding and cutting (and also by random RNase contamination), incubation of TB-RBP with the 500 bp dsRNA in a stoichiometric manner resulted mainly in the equivalent amount of the ∼25 bp fragments and a product whose molecular weight is slightly smaller than 500 bp, most likely the 450 bp product (Figures 4 and 6). On the other hand, when a large excess of protein was used to cut ssRNA or dsRNA, complete digestion of the nucleic acids was achieved because, when the protein−product complex leaves, the open ends of the nucleic acids are ready for the next protein molecule to bind (Figure 5).

The high product−protein affinity implies an in vivo regulatory mechanism instructing the protein to bind to its targets when needed and to release the products when necessary. This regulation could be achieved by the organization of the protein itself (such as different forms of octamers) or, more likely, by other regulating proteins that interact with TB-RBP. In fact, the X-ray structure shows that the octamer organization of the protein provides a large surface for binding other proteins (regulators) (*43*). TRAX is so far the only TB-RBP/translin binding protein described, and it could serve as one of the regulators. Although controversial, it has been reported that, upon binding to TB-RBP/translin, it lowers RNA-binding affinity of the latter (*51*). We are currently involved in determining which proteins can interact and regulate TB-RBP/translin.

Overall, using the photoaffinity method, we found that TB-RBP/translin binds strongly to siRNA. Whether TB-RBP/translin is a component of RISC and is involved in RNAi remains to be addressed. Nevertheless, we discovered that this protein possesses both ssRNase and dsRNase activities that process the nucleotides into ∼25 bp products. However, due to its high affinity for ∼25 bp products, product inhibition causes the protein to exhibit a very low turnover number. Therefore, under physiological conditions, the binding affinity between TB-RBP/translin and short (∼25 bp) dsRNA must be regulated. Furthermore, this newly discovered activity, together with the reported functions (see the introduction), suggests that TB-RBP/translin must be tightly regulated with respect to it activities and translocation. While regulatory mechanisms of these activities are still being sought, the finding opens a new vista for studying the protein behavior in vivo: downstream events of tight protein−nucleic acid binding.

ACKNOWLEDGMENT

We thank Mr. Eric Schneider for preparing the *E. coli* expressing His-tagged TB-RBP.

REFERENCES

1. Tijsterman, M., Ketting, R. F., and Plasterk, R. H. A. (2002) The genetics of RNA silencing, *Annu. Rev. Genet. 36*, 489−519.
2. Zamore, P. D. (2001) RNA interference: listening to the sound of silence, *Nat. Struct. Biol. 8*, 746−750.
3. Hannon, G. J. (2002) RNA interference, *Nature 418*, 244−251.
4. Dykxhoom, D. M., Novina, C. D., and Sharp, P. A. (2003) Killing the messenger: short RNAs that silence gene expression, *Nat. Rev. Mol. Cell Biol. 4*, 457−467.
5. Carpenter, A. E., and Sabatini, D. M. (2004) Systematic genome-wide screens of gene function, *Nat. Rev. Genet. 5*, 11−22.
6. Voorhoeve, P. M., and Agami, R. (2003) Knockdown stands up, *Trends Biotechnol. 21*, 2−4.
7. Caplen, N. J. (2003) RNAi as a gene therapy approach, *Expert Opin. Biol. Ther. 3*, 575−586.
8. Arenz, C., and Schepers, U. (2003) RNA interference: from an ancient mechanism to a state of the art therapeutic application?, *Naturwissenschaften 90*, 345−359.
9. Kennerdell, J. R., and Carthew, R. W. (1998) Use of dsRNA-mediated genetic interference to demonstrate that *frizzled* and *frizzled 2* act in the wingless pathway, *Cell 95*, 1017−1026.
10. Misquitta, L., and Paterson, B. M. (1999) Targeted disruption of gene function in *Drosophila* by RNA interference (RNA-i): A role for *nautilus* in embryonic somatic muscle formation, *Proc. Natl. Acad. Sci. U.S.A. 96*, 1451−1456.
11. Fraser, A. G., Kamath, R. S., Zipperlen, P., Martinez-Campos, M., Sohrmann, M., and Ahringer, J. (2000) Functional genomic analysis of *C. elegans* chromosome I by systematic RNA interference, *Nature 408*, 325−330.
12. Gonczy, P., Echeverri, C., Oegema, K., Coulson, A., Jones, S. J., Copley, R. R., Duperon, J., Oegema, J., Brehm, M., Cassin, E., Hannk, E., Kirkham, M., Pichler, S., Flohrs, K., Goessen, A., Leidel, S., Alleaume, A.-M., Martin, C., Ozlu, N., Bork, P., and Hyman, A. A. (2000) Functional genomic analysis of cell division in *C. elegans* using RNAi of genes on chromosome III, *Nature 408*, 331−336.
13. Elbashir, S. M., Harborth, J., Lendeckel, W., Yalcin, A., Weber, K., and Tuschl, T. (2001) Duplexes of 21-nucleotide RNAs mediate RNA interference in cultured mammalian cells, *Nature 411*, 494−498.
14. Brummelkamp, T. R., Bernard, R., and Agami, R. (2002) A system for stable expression of short interfering RNAs in mammalian cells, *Science 296*, 550−553.
15. Sui, G., Soohoo, C., Affar, El B., Gay, F., Shi, Y., Forrester, W. C., and Shi, Y. A. (2002) A DNA vector-based RNAi technology to suppress gene expression in mammalian cells, *Proc. Natl. Acad. Sci. U.S.A. 99*, 5515−5520.
16. Oubrahim, H., Chock, P. B., and Stadtman, E. R. (2002) Manganese(II) induces apoptotic cell death in NIH3T3 cells via a Caspase-12-dependent pathway, *J. Biol. Chem. 277*, 20135−20138.
17. Wang, J., Tekle, E., Oubrahim, H., Mieyal, J. J., Stadtman, E. R., and Chock, B. P. (2003) Stable and controllable RNA interference: Investigating the physiological function of glutathionylated actin, *Proc. Natl. Acad. Sci. U.S.A. 100*, 5103−5106.
18. Seldz, C. A., Holko, M., de Veer, M. J., Silverman, R. H., and Williams, B. R. G. (2003) Activation of the interferon system by short-interfering RNAs, *Nat. Cell Biol. 5*, 834−839.
19. Bartel, D. P. (2004) MicroRNAs: genomics, biogenesis, mechanism, and function, *Cell 116*, 281−297.
20. Carrington, J. C., and Ambros, V. (2003) Role of microRNAs in plant and animal development, *Science 301*, 336−338.
21. Moor, M. J. (2002) Nuclear RNA turnover, *Cell 108*, 431−434.
22. Agrawal, N., Dasaradhi, P. V., Mohmmed, A., Malhotra, P., Bhatnagar, R. K., and Mukherjee, S. K. (2003) RNA interference: biology, mechanism, and applications, *Microbiol. Mol. Biol. Rev. 67*, 657−685.

23. Schwarz, D. S., Hutvagner, G., Du, T., Xu, Z., Aronin, N., and Zamore, P. D. (2003) Asymmetry in the assembly of the RNAi enzyme complex, *Cell 115*, 199−208.
24. Lipardi, C., Wei, Q., and Paterson, B. M. (2001) RNAi as random degradative PCR: siRNA primers convert mRNA into dsRNAs that are degraded to generate new siRNAs, *Cell 107*, 297−307.
25. Hmmond, S. M., Boettcher, S., Caudy, A. A., Kobayashi, R., and Hannon, G. J. (2001) Argonaute2, a link between genetic and biochemical analyses of RNAi, *Science 293*, 1146−1150.
26. Song, J. J., Liu, J., Tolia, N. H., Schneiderman, J., Smith, S. K., Martienssen, R. A., Hannon, G. J., and Joshua-Tor, L. (2003) The crystal structure of the Argonaute2 PAZ domain reveals an RNA binding motif in RNAi effector complexes, *Nat. Struct. Biol. 10*, 1026−1032.
27. Kwon, K. Y., and Hecht, N. B. (1991) Cytoplasmic protein binding to highly conserved sequences in the 3′ untranslated region of mouse protamine 2 mRNA, a translationally regulated transcript of male germ cells, *Proc. Natl. Acad. Sci. U.S.A. 88*, 3584−3588.
28. Kwon, K. Y., and Hecht, N. B. (1993) Binding of a phosphoprotein to the 3′ untranslated region of the mouse protamine 2 mRNA temporally represses its translation, *Mol. Cell. Biol. 13*, 6547−6557.
29. Wu, X.-Q., and Hecht, N. B. (2000) Mouse testis brain ribonucleic acid-binding protein/translin colocalizes with microtubules and is immunoprecipitated with messenger ribonucleic acids encoding myelin basic protein, α calmodulin kinase II, and protamines 1 and 2, *Biol. Reprod. 62*, 720−725.
30. Finkenstadt, P. M., Jeon, M., and Baraban, J. M. (2001) Masking of the translin/Trax complex by endogenous RNA, *FEBS Lett. 498*, 6−10.
31. Aoki, K., Suzuki, K., Sugano, T., Tasaka, T., Nakahara, K., Kuge, O., Omori, A., and Kasai, M. (1995) A novel gene, translin, encodes a recombination hotspot binding protein associated with chromosomal translocations, *Nat. Genet. 10*, 167−174.
32. Badge, R. M., Yardley, J., Jeffreys, A. J., and Armour, J. A. (2000) Crossover breakpoint mapping identifies a subtelomeric hotspot for male meiotic recombination, *Hum. Mol. Genet. 9*, 1239−1244.
33. Aoki, K., Suzuki, K., Ishida, R., and Kasai, M. (1999) The DNA binding activity of translin is mediated by a basic region in the ring-shaped structure conserved in evolution, *FEBS Lett. 443*, 363−366.
34. Kasai, M., Matsuzaki, T., Katayanagi, K., Omori, A., Maziarz, R. T., Strominger, J. L., Aoki, K., and Suzuki, K. (1997) The translin ring specifically recognizes DNA ends at recombination hot spots in the human genome, *J. Biol. Chem. 272*, 11402−11407.
35. Wu, W.-Q., Gu, W., Meng, X.-H., and Hecht, N. B. (1997) The RNA-binding protein, TB-RBP, is the mouse homologue of translin, a recombination protein associated with chromosomal translocations, *Proc. Natl. Acad. Sci. U.S.A. 94*, 5640−5645.
36. Han, J. R., Gu, W., and Hecht, N. B. (1995) Testis-brain RNA-binding protein, a testicular translational regulatory RNA-binding protein, is present in the brain and binds to the 3′ untranslated regions of transported brain mRNAs, *Biol. Reprod. 53*, 707−717.
37. Han, J. R., Yiu, K. C., and Hecht, N. B. (1995) Testis/brain RNA-binding protein attaches translationally repressed and transported mRNAs to microtubules, *Proc. Natl. Acad. Sci. U.S.A. 92*, 9550−9554.
38. Morales, C. R., Wu, X.-Q., and Hecht, N. B. (1998) The DNA/RNA-binding protein, TB-RBP, moves from the nucleus to the cytoplasm and through intercellular bridges in male germ cells, *Dev. Biol. 201*, 113−123.
39. Morales, C. R., Lefrancois, S., Chennathukuzhi, V., El-Alfy, M., Wu, X.-Q., Yang, J., Gerton, G. L., Moss, S. B., and Hecht, N. B. (2002) A TB-RBP and Ter ATPase complex accompanies specific mRNAs from nuclei through the nuclear pores and into intercellular bridges in mouse male germ cells, *Dev. Biol. 246*, 480−494.
40. Lee, P. S., Fuior, E., Lewis, M. S., and Han, M. K. (2001) Analytical ultracentrifugation studies of translin: Analysis of protein-DNA interactions using a single-stranded fluorogenic oligonucleotide, *Biochemistry 40*, 14081−14088.
41. Sengupta, K., and Rao, B. J. (2002) Translin binding to DNA: recruitment through DNA ends and consequent conformational transitions, *Biochemistry 41*, 15315−15326.
42. VanLoock, M. S., Yu, X., Kasai, M., and Egelman, E. H. (2001) Electron microscopic studies of the translin octameric ring, *J. Struct. Biol. 135*, 58−66.
43. Pascal, J. M., Hart, J. P., Hecht, N. B., and Robertus, J. D. (2002) Crystal structure of TB-RBP, a novel RNA-binding and regulating protein, *J. Mol. Biol. 319*, 1049−1057.
44. Han, M. K., Lin, P., Paek, D., Harvey, J. J., Fuior, E., and Knutson, J. R. (2002) Fluorescence studies of pyrene maleimide-labeled translin: excimer fluorescence indicates subunits associate in a tail-to-tail configuration to form octamer, *Biochemistry 41*, 3468−3476.
45. Chennathukuzhi, V. M., Kurihara, Y., Bray, J. D., Yang, J., and Hecht, N. B. (2001) Altering the GTP binding site of the DNA/RNA-binding protein, translin/TB-RBP, decreases RNA binding and may create a dominant negative phenotype, *Nucleic Acids Res. 29*, 4433−4440.
46. Chennathukuzhi, V., Stein, J. M., Abel, T., Donlon, S., Yang, S., Miller, J. P., Allman, D. M., Simmons, R. A., and Hecht, N. B. (2003) Mice deficient for testis-brain RNA-binding protein exhibit a coordinate loss of TRAX, reduced fertility, altered gene expression in the brain, and behavioral changes, *Mol. Cell. Biol. 23*, 6419−6434.
47. Yang, S., Cho, Y.-S., Chennathukuzhi, V. M., Underkoffler, L. A., Loomes, K., and Hecht, N. B. (2004) Translin-associated factor X is post-transcriptionally regulated by its partner protein TB-RBP, and both are essential for normal cell proliferation, *J. Biol. Chem. 279*, 12605−12614.
48. Finkenstadt, P. M., Jeon, M., and Baraban, J. M. (2002) Trax is a component of the translin-containing RNA binding complex, *J. Neurochem. 83*, 202−210.
49. Boja, E. S., Hoodbhoy, T., Fales, H. M., and Dean, J. (2003) Structural characterization of native mouse zona pellucida proteins using mass spectrometry, *J. Biol. Chem. 278*, 34189−34202.
50. Fourrey, J. L., Jouin, P., and Moron, J. (1974) Thiocarbonyl photochemistry. III. thietanes obtention from 4-thiouracil derivatives, *Tetrahedron Lett. 35*, 3005−3006.
51. Chennathukuzhi, V., Kurihara, Y., Bray, J. D., and Hecht, N. B. (2001) Trax (translin-associated factor X), a primarily cytoplasmic protein, inhibits the binding of TB-RBP (translin) to RNA, *J. Biol. Chem. 276*, 13259−13262.

BI048847L